ELSEVIER

SCIENCE DIRECT®

PHYSICS LETTERS B

Physics Letters B 553 (2003) 217–222

www.elsevier.com/locate/npe

Hadron multiplicity in lepton–nucleon interactions

G.I. Lykasov [a], U. Sukhatme [b], V.V. Uzhinsky [a]

[a] *Joint Institute for Nuclear Research, Dubna, Moscow Region, 141980, Russia*
[b] *State University of New York at Buffalo, 810 Clemens Hall, Buffalo, NY 14260-4600, USA*

Received 15 November 2002; accepted 13 December 2002

Editor: G.F. Giudice

Abstract

Multi-hadron production in inelastic neutrino–nucleon interactions is investigated within the framework of the quark–gluon string model. The contributions of the planar (one-reggeon exchange) and cylindrical (one-pomeron exchange) graphs to different observables is computed using a Monte Carlo program for the generation of hadrons produced from the decay of colorless quark–antiquark strings. The suggested approach results in a satisfactory description of the experimental data on $\nu(\bar{\nu})N \to \mu^-(\mu^+)hX$ reactions obtained recently at CERN by the NOMAD Collaboration. The data extends over a wide range of initial neutrino energies $E_\nu < 200$ GeV/c and momentum transfers $1 < Q < 7$ GeV/c, well into the region where perturbative QCD calculations are not applicable.

PACS: 13.60.Le; 13.60.Hb

The investigation of multi-hadron production in inelastic lepton–nucleon interactions is a tool to study the dynamics of such processes and the nucleon structure function, particularly the Q^2 dependence over a wide interval of values. In analyzing these types of reactions, the fragmentation properties of the struck quark in deep inelastic scattering (DIS) in $\nu_\mu N$ and $\bar{\nu}_\mu N$ charged current events are often compared to those of the quarks produced in e^+e^- annihilation and ep inelastic scattering. This comparison tests the universality of the quark fragmentation process in regions where non-perturbative QCD effects are important. Such an analysis has been performed recently in Ref. [1]. It has also been found that a perturbative QCD calculation results in a good description of the charged hadron multiplicity $\langle n_{\rm ch}\rangle$ measured in e^+e^- annihilation and ep DIS at initial energies $E = \sqrt{s} = Q > 5$ GeV/c [1], whereas a similar calculation of $\langle n_{\rm ch}\rangle$ in the current region of processes $\nu(\bar{\nu})p \to \mu^-(\mu^+)hX$ cannot reproduce the NOMAD data at $Q < 5$ GeV/c. This discrepancy is an important motivation for the present analysis of inelastic neutrino–nucleon interactions within the framework of the quark–gluon string model (QGSM) [2, 3], which is essentially equivalent to the dual parton model (DPM) developed in Refs. [4,5]. We calculate the different observables in a manner similar to Ref. [6], which focused on the pion multiplicity in $\nu(\bar{\nu})A \to \mu^-(\mu^+)hX$ reactions. The main difference from the previous study is that we now use the Monte Carlo (MC) generation of hadrons produced from the

E-mail address: lykasov@sissa.it (G.I. Lykasov).

0370-2693/02
doi:10.1016/S0370-2693(02)03225-2

decay of colorless strings. This procedure allows us to analyze all the observables measured experimentally and make a comparison with recent data [1].

In the QGSM [2,3], hadron production in the reactions $\nu(\bar{\nu})p \to \mu^-(\mu^+)hX$ is described in terms of planar and cylindrical graphs, as shown in Fig. 1. The planar graph of Fig. 1(a) describes neutrino scattering off a valence quark, corresponding to the one-reggeon exchange in the t-channel [2], whereas the cylindrical graph of Fig. 1(b) describes neutrino scattering off sea quarks in the proton corresponding to the one-pomeron exchange in the t-channel [2]. The figures also show the occurrence of hadronization in the colorless quark–antiquark and quark–diquark strings.

The relativistic invariant distribution of hadrons produced in the process $\nu(\bar{\nu})p \to \mu^-(\mu^+)hX$ is defined as

$$\rho_{\nu(\bar{\nu})p\to\mu^-(\mu^+)hX} = E_h \frac{dN}{d^3p_h\, d\Omega\, dE'}, \tag{1}$$

where E_h and $\mathbf{p}_h$ are the total energy and three momentum of the produced hadron, respectively; E' and Ω are the energy and the solid angle of the final muon. It can be written in the following general form

$$\rho_{\nu(\bar{\nu})p\to\mu^-(\mu^+)hX} = \Phi(Q^2)\left\{F_P\left(x, Q^2; z, p_{\rm ht}\right) + F_C\left(x, Q^2; z, p_{\rm ht}\right)\right\} \tag{2}$$

with

$$\Phi\left(Q^2\right) = mE\frac{G^2}{\pi}\frac{m_W^2}{Q^2+m_W^2},$$

where G is the Fermi weak coupling constant, E is the energy of the incoming neutrino, m and m_W are the nucleon and the W-boson masses, respectively, $x = Q^2/2(p_\nu \cdot k)$ is the Bjorken variable, p_ν and k are the four momenta of the initial neutrino and nucleon. Here $F_P(x, Q^2; z, p_{\rm ht})$ and $F_C(x, Q^2; z, p_{\rm ht})$ are the probability distributions of produced hadrons corresponding to the planar and cylindrical graphs of Fig. 1, respectively. The contributions F_P and F_C are computed by using the MC generation of all the quark–antiquark and quark–diquark strings drawn in Fig. 1(a) and (b). Generally, z is the light cone variable defined as $z = (E_h + p_{hz})/(E + p_z)$, where p_{hz} is the hadron longitudinal momentum respect to the initial neutrino having momentum p_z, see for example, Refs. [2–5]. At large energies of final hadrons it is the longitudinal momentum fraction of hadron with respect to the neutrino in the rest frame of the proton-target. The variable z can be treated also as the Feynman variable $x_F = 2p_L^*/W_X$ defined as the longitudinal momentum fraction in the hadronic center of mass system (h.c.m.s.). Here p_L^* is the longitudinal hadron momentum in the h.c.m.s., W_X is the mass of hadrons produced in the reaction, then $p_{\rm ht}$ is the transverse momentum of produced hadron with respect to the current (hadronic jet) direction, see, for example, Ref. [7].

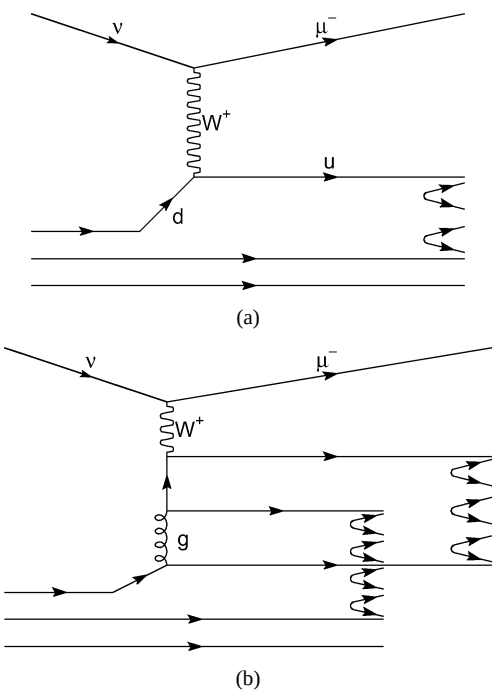

Fig. 1. (a) The planar (one-reggeon exchange) graph and (b) the cylindrical (one-pomeron exchange) graph.

The main ingredients for the calculations of observables in the discussed reaction are the quark distributions in a nucleon and their fragmentation functions to hadrons. In addition to the dependence upon x, quark distributions also depend on Q^2 and the transverse momentum k_t. Following Ref. [6], we take a factorized form for these distributions:

$$q_f\left(x, Q^2; k_t\right) = q_f\left(x, Q^2\right)g_q(k_t), \tag{3}$$

with the function g_q chosen in the form

$$g_q(k_t) = \frac{B^2}{2\pi} e^{-Bk_t}, \tag{4}$$

where $B = 1/\langle k_t \rangle \simeq 4\ (\mathrm{GeV}/c)^{-1}$, and $\langle k_t \rangle \simeq 0.25$ GeV/c is the average transverse momentum of a quark in a nucleon. As for the function $q_f(x, Q^2)$ we use the fit suggested in Ref. [8] including the true Regge x-asymptotic at $x \to 0, x \to 1$ and small Q^2, and its QCD prediction at large Q^2. More specifically, the valence u and d quark distributions according to Ref. [8], have the following forms:

$$q_u\big(x, Q^2\big) = B_u x^{-\alpha_R(0)} (1-x)^{n(Q^2)} \left(\frac{Q^2}{Q^2+b}\right)^{\alpha_R(0)}, \tag{5}$$

$$q_d\big(x, Q^2\big) = B_d x^{-\alpha_R(0)} (1-x)^{n(Q^2)+1} \left(\frac{Q^2}{Q^2+b}\right)^{\alpha_R(0)}, \tag{6}$$

where

$$n\big(Q^2\big) = \frac{3}{2}\left(1 + \frac{Q^2}{Q^2+c}\right).$$

We take the values of the constants from Ref. [8]: a $\alpha_R(0) = 0.4150$ is the reggeon intercept, $B_u = 1.2064$, $B_d = 0.1798$, $b = 0.6452$, $c = 3.5489$.

The sea quark distribution in the proton is taken to be [8]:

$$q_{\mathrm{sea}}\big(x, Q^2\big) = A x^{-\Delta(Q^2)-1} (1-x)^{n(Q^2)+4} \left(\frac{Q^2}{Q^2+a}\right)^{1+\Delta(Q^2)}, \tag{7}$$

where

$$\Delta\big(Q^2\big) = \Delta_0\left(1 + \frac{\Delta_1(Q^2) \times Q^2}{Q^2+\Delta_2}\right),$$

and $A = 0.1502$, $a = 0.2631$, $\Delta_0 = 0.07684$, $\Delta_1 = 2.0$, $\Delta_2 = 1.1170$. Note, this fit of the quark distributions in the proton describes all the experimental data from very small x up to $x \sim 0.9$ [8].

Generally, the fragmentation functions (FF) of quarks (diquarks) $D^h_{q(qq)}$ into hadrons depend on the hadron momentum fraction z_1 and the hadron transverse momentum $\tilde{p}_{\mathrm{ht}}$ with respect to a quark (diquark) momentum direction. Here also we choose the factorized form

$$D^h_{q(qq)}(z_1, k_t) = D^h_{q(qq)}(z_1) g_q(\tilde{p}_{\mathrm{ht}}), \tag{8}$$

with the function g_q again chosen in the form (4). The functions $D^h_{q(qq)}(z_1)$ are constructed, according to the recursive cascade model procedure suggested in [9]. They are found from the following integral equation [9]:

$$D^h_{q(qq)}(z_1) = f(z_1) + \int_{z_1}^{1} f(x) D^h_{q(qq)}\left(\frac{z_1}{x}\right)\frac{dx}{x}. \tag{9}$$

The function $f(x)$ is chosen in the form

$$f(x) = x^{\beta}(1-x)^{\gamma}. \tag{10}$$

According to the main points of the QGSM, the fragmentation functions $D^h_{q(qq)}(z_1)$ should satisfy true Regge asymptotics at $z_1 \to 1$ and $z_1 \to 0$ [3]. This limitation allows us to find the values of the parameters. The detailed procedure is presented in Ref. [10]. In general case the FF have to depend not only on z_1, p_{ht} but also on Q^2. At small Q^2 they have to reproduce the true Regge asymptotic [3] and at large Q^2 they have to describe the e^+e^- annihilation data. Since we analyze inelastic neutrino- nucleon interactions mainly at not large Q^2, one can assume that the FF depends on it weakly and neglect this Q^2 behaviour of $D^h_{q(qq)}$.

The MC computation results of the different observables in the reaction $\nu + N \to \mu^- + h + X$ are presented in Figs. 2–5. The mean charged multiplicity in the current region is presented in Fig. 2. As it shown in [1] the NOMAD multiplicity values n_{ch} are very close to $\langle n_{\mathrm{ch}} \rangle/2$ results from e^+e^- experiment [11] at energy $E = \sqrt{s}$ and $\langle n_{\mathrm{ch}} \rangle$ from ep and $\bar{\nu}_\mu p$ at $E = Q$. In Fig. 2 we compare our results with the QCD calculation of the charged multiplicity from e^+e^- $\langle n^{\mathrm{QCD}}_{\mathrm{ch}} \rangle/2$. The open circles in Fig. 2 correspond to the QCD calculations [12,13] for the evolution of partons in the leading log approximation which give for $\langle n^{\mathrm{QCD}}_{\mathrm{ch}} \rangle$ the following fit, see also [1,14],

$$n^{\mathrm{QCD}}_{\mathrm{ch}} = a + b \exp\left(c\sqrt{\ln\big(Q^2/Q_0^2\big)}\right), \tag{11}$$

where $a = 2.257$, $b = 0.094$, $c = 1.775$, $Q_0 = 1$ GeV/c. The solid, long dash and short dash lines in Fig. 2 correspond to our Monte Carlo calculation at the initial neutrino energies $E_\nu = 150$ GeV, $E_\mu = 45$ GeV,

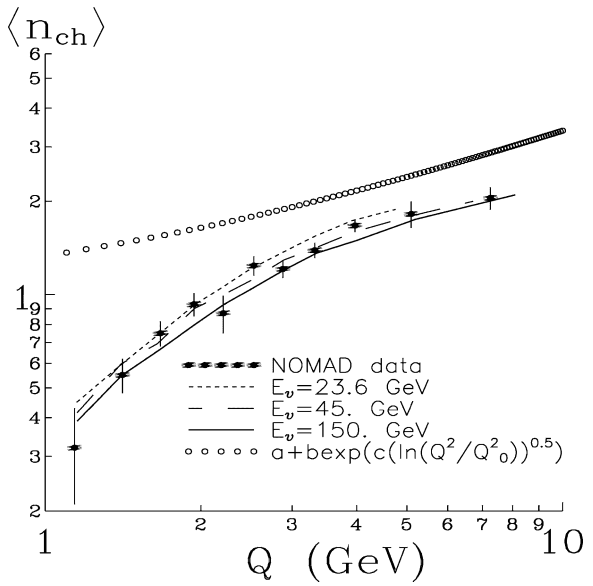

Fig. 2. Mean multiplicity of charged hadrons in the current fragmentation region as a function of the momentum transfer Q. The open circles correspond to the QCD fit given by Eq. (11); the solid, long dash and short dash lines correspond to our calculations at $E_\nu = 150$ GeV, 45 GeV and $E_\nu = 23.64$ GeV, respectively. The experimental points are the NOMAD data [1].

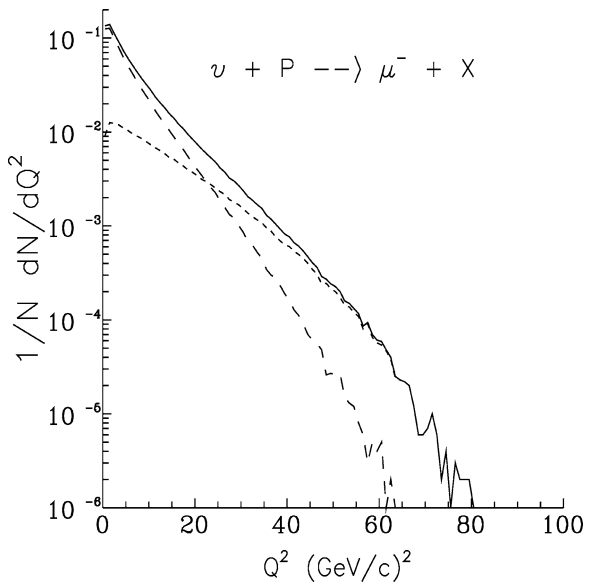

Fig. 3. The Q^2-distribution $1/NdN/dQ^2$ of muons produced in the inclusive process $\nu + p \to \mu^- + X$. The long dash and short dash lines correspond to the contributions of the cylindrical and planar graphs, respectively. The solid line is the sum of these contributions.

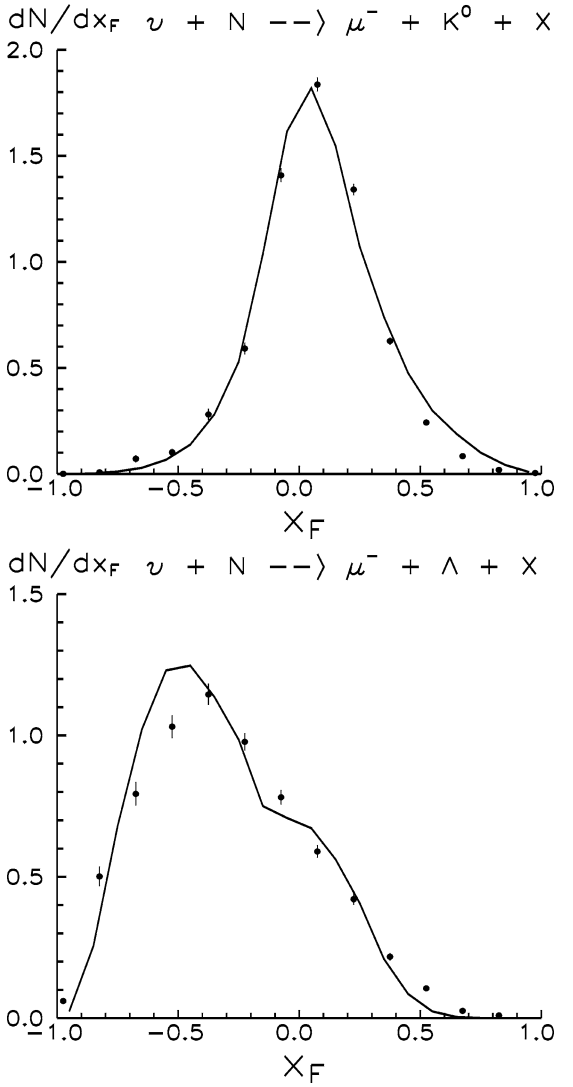

Fig. 4. The x_F distribution of strange hadrons. The upper panel corresponds to the distribution dN/x_F of K^0 mesons in semi-inclusive process $\nu + N \to \mu^- + K^0 + X$, whereas the lower panel shows the x_F distribution of Λ^0 hyperons produced in $\nu + N \to \mu^- + \Lambda^0 + X$ reaction. The experimental points are the NOMAD data [1].

$E_\nu = 23.6$ GeV, respectively. The NOMAD experimental data are averaged over the initial energy [1]. It is seen from Fig. 1 that the QCD fit cannot reproduce the NOMAD data on the charged multiplicity at $Q < 5$ GeV/c, whereas at large Q it describes these ones and $\langle n_{\rm ch}\rangle$ from e^+e^-, ep and $\bar{\nu}_\mu p$ experiments satisfactory as it is shown in [1]. The suggested ap-

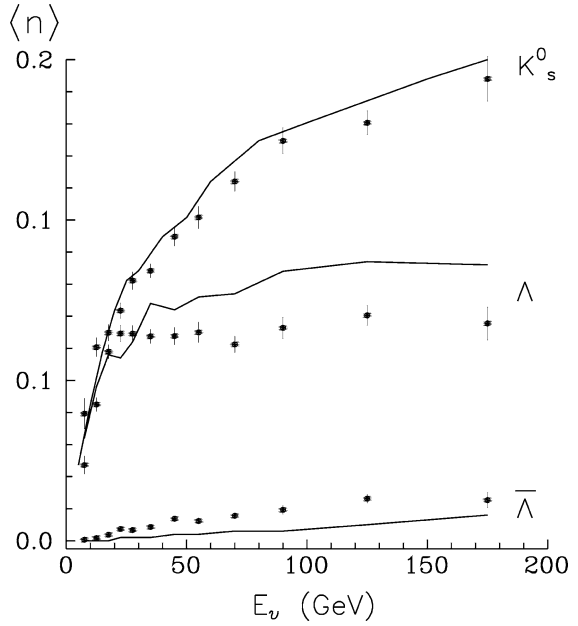

Fig. 5. The average multiplicity of the strange hadrons as a function of the neutrino energy E_ν. The upper line corresponds to $\langle n\rangle$ of the K^0_s mesons, the middle line is the mean multiplicity of Λ^0 hyperons and the down curve shows $\langle n\rangle$ of the antilambda hyperons $\bar{\Lambda}^0$.

proach describes the NOMAD data at $Q < 5$ GeV/c rather well.

In Fig. 3 the Q^2 dependence of the inclusive muon spectrum in the process $\nu + p \to \mu^- + X$ is presented. The long and the short dash lines correspond to the contributions of the cylindrical (one-pomeron exchange) and the planar (one-reggeon exchange) graphs to this spectrum, the solid line shows their incoherent sum. It is seen from Fig. 3 that the contribution of the one-pomeron exchange graph is decreasing with increase of Q^2 much faster than the one of the one-reggeon diagram which dominates at $Q^2 > 20$ (GeV/c)^2.

In Fig. 4 the x_F distributions of strange K^0-mesons and Λ-baryons are presented. The solid lines in Fig. 3 correspond to our calculation, the experimental points are the NOMAD data [7]. This figure shows rather satisfactory description of the NOMAD data.

In Fig. 5 our calculation results of the mean multiplicity of the strange hadrons K^0_S, Λ and $\bar{\lambda}$ as the function of the neutrino energy E_ν with the NOMAD data [7] are presented.

In this Letter we have analyzed the multiple hadron production in inelastic neutrino–nucleon processes. The main conclusions of our work can be summarized as follows. By the analysis of the charged hadron multiplicity in the current region of the process $\nu + p \to \mu^- + h + X$ at $Q^2 \leqslant 10$ (GeV/c)^2 the nonperturbative QCD effects become very important. The conventional perturbative QCD calculation of $\langle n_{\rm ch}\rangle$ does not reproduce the NOMAD data in this region, whereas the application of the QGSM or the DPM allows to describe these data rather satisfactory. The main contribution to this observable and the muon distribution $1/N d\sigma/dQ^2$ at small Q^2 is coming from the cylindrical (one-pomeron exchange) graph, Fig. 1(b), whereas at large Q^2 the planar (one-reggeon) graph, Fig. 1(a), dominates. Note, these two observables presented in Figs. 2, 3 are related to the current fragmentation region. Recently in [6] it has been shown that in the target fragmentation region these two contributions to the multiplicity of pions produced in the backward hemisphere in inelastic neutrino–nucleus collisions have the Q^2 dependences opposite to the ones obtained in this Letter. There is some analogous between the last reaction and the soft $h - N$ processes at $x_F \to -1$ when the one-pomeron exchange graph dominates at large initial energy, see for example [2]. Therefore, the contributions of Fig. 1(a) and (b) graphs have different Q^2 dependences in the different kinematical regions, the current and the target fragmentation ones.

The NOMAD data on the x_F distributions of strange hadrons are described by the QGSM rather satisfactorily. It can mean that the fragmentation functions of quarks (diquarks) used by description of soft h–N processes are rather good to analyse the multiple hadron production in inelastic ν–N interactions at not large Q^2.

Acknowledgements

We are indebted to A.B. Kaidalov, B. Popov and A. Capella for many helpful discussions. One of the authors (V.V.U.) thanks RFBR, grant No. 00-01-00307, and INTAS, grant No. 00-00366, for their financial support. Support from the US Department of Energy is gratefully acknowledged.

References

[1] NOMAD Collaboration, J. Altegoer, et al., Phys. Lett. B 445 (1999) 439.
[2] A.B. Kaidalov, Sov. J. Nucl. Phys. 33 (1981) 733.
[3] A.B. Kaidalov, Phys. Lett. B 116 (1982) 459;
A.B. Kaidalov, Sov. J. Nucl. Phys. 45 (1987) 902.
[4] A. Capella, U. Sukhatme, C.I. Tan, J. Tran Thanh Van, Phys. Lett. B 81 (1979) 68;
A. Capella, U. Sukhatme, C.I. Tan, J. Tran Thanh Van, Z. Phys. 63 (1979) 68.
[5] A. Capella, U. Sukhatme, C.I. Tan, J. Tran Thanh Van, Phys. Rep. 236 (1994) 223.
[6] O. Benhar, S. Fantoni, G.I. Lykasov, U. Sukhatme, Phys. Lett. B 527 (2002) 73.
[7] NOMAD Collaboration, P. Astier, Nucl. Phys. B 621 (2002) 3.
[8] A. Capella, A. Kaidalov, C. Merino, J. Tran Thanh Van, Phys. Lett. B 337 (1994) 358;
A. Capella, A. Kaidalov, C. Merino, J. Tran Thanh Van, Phys. Lett. B 343 (1995) 403;
A. Kaidalov, C. Merino, Eur. Phys. J. C 10 (1999) 153.
[9] R.D. Field, R.P. Feynman, Nucl. Phys. B 136 (1978) 1;
U. Sukhatme, Phys. Lett. B 73 (1978) 478;
U. Sukhatme, Z. Phys. C 2 (1979) 321;
U. Sukhatme, K. Lassila, R. Orava, Phys. Rev. D 25 (1982) 2975.
[10] V.V. Uzhinsky, S.Yu. Shmakov, Sov. J. Nucl. Phys. 53 (1991) 1034.
[11] JADE Collaboration, W. Bartel, et al., Z. Phys. C 20 (1983) 187.
[12] W. Furmanski, R. Petronzio, S. Pokorski, Nucl. Phys. B 155 (1979) 253.
[13] A. Bassetto, M. Ciafaloni, G. Marchesini, Phys. Lett. B 83 (1979) 207;
K. Konishi, Rutherford Report RL 79-035, 1979;
A.H. Mueller, Phys. Lett. B 104 (1981) 161;
A.H. Mueller, Nucl. Phys. B 213 (1983) 85.
[14] TASSO Collaboration, W. Braunschweig, et al., Z. Phys. C 45 (1989) 194.